

# Recent Advances in Iridology based Disease Detection: A Comprehensive Review

Alaa Abdulkareem Ahmed\*, Mohammad Tariq Yaseen\*\*

\* Department of Electrical Engineering, College of Engineering, University of Mosul, Mosul, Iraq  
Email: alaa.22enp39@student.uomosul.edu.iq  
<https://orcid.org/0009-0004-4446-4015>

\*\* Department of Electrical Engineering, College of Engineering, University of Mosul, Mosul, Iraq  
Email: mtyaseen@uomosul.edu.iq  
<https://orcid.org/0000-0001-7173-8684>

## Abstract

The increasing demand for non-invasive, rapid, and cost-effective disease diagnostics has driven advancements in integrating Iridology with computer vision and Artificial Intelligence (AI). This review examines research conducted from 2009 to 2024 on iris-based disease detection. The key findings showed the significant role of Machine Learning (ML) and Deep Learning (DL) in enhancing diagnostic accuracy and efficiency. Iridology-based intelligent systems show great promise for early detection of hidden diseases and organ dysfunctions, offering transformative potential for healthcare.

**Keywords-** Iridology, Disease, Region of Interest (ROI), Artificial Intelligence (AI), Machine Learning (ML).

## I. INTRODUCTION

An eye's iris is interconnected with a large number of minute nerve filaments, which receive messages from every nerve in the body via optic nerves, optic thalami, and spinal cord [1]. The signals sent from the body's organs are recorded in the brain; since the iris is directly connected to the brain, the signals are also recorded in the iris [2]. Changes in organ conditions are replicated by nerve filaments, muscle fibers, and minute blood vessels in different areas of the iris. Clinical information is obtained by examining various marks, signs, abnormal colors, or discolorations in the iris. These symptoms, marks, and stains are indicative of acute and chronic inflammatory or catarrhal conditions, local lesions, tissue damage, various drug poisons, and structural and tissue changes caused by accidental injury or surgical mutilation[1]. Therefore, since the iris is where the nervous systems are located, it is a data screen to give information about the human body, which is called Iris diagnostics (Iridology) [3]. The location of the iris can be observed according to the anatomy of the eye as shown in Figure 1 below [4].

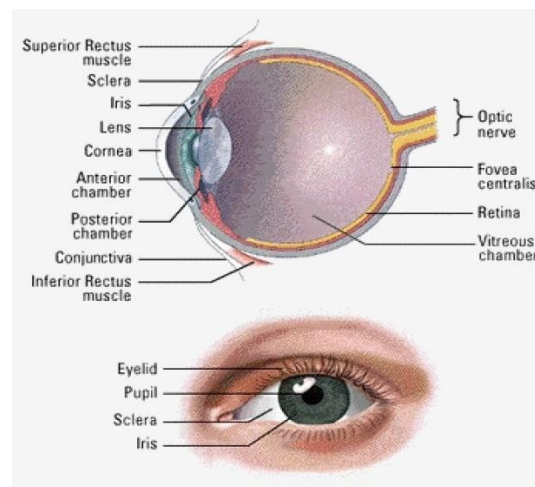


Figure1. Anatomy of Human Eye Iris. [4]

The study of the iris is called Iridology and is referred to as a map of the human body [5]. And it is one of the sciences of complementary and alternative medicine (CAM) that shows that the pattern of the iris can reflect the state of health of the body's organs [4]. It can be said that it does not diagnose any disease, but it reveals a weakness in a certain part of the human body with the eye corresponding to that organ's location the body [6]. It can also be classified as a new path of medical diagnosis because there is no touch, no pain, or no damage and it has high accuracy [3], But this science has an ancient history of more than 3000 years, it has a long history in India in Tibet to examine the disease, the first person to find Iridology was Dr. Ignatz von Peczely more than 1800 years ago [7]. Dr. Peczely drew the first iris chart as a result of studying the changes in the eyeballs and iris of patients. Since then, iris has evolved in Taiwan, developing iridescence in 1988, after the Chinese version of the book "Science and Practice of Iridology" was published by Dr. Chung of the General Hospital of Veterans, written by American iridescent Dr. Berward Jensen [7]. After the research work by the doctors and iridology specialists, all the organs of the body were represented in the diagram of the iris chart to diagnose human health by interpreting the patterns of the iris. The computer was used in iris diagnostics because it analyzes pattern images [3].

The iris globally is topographically described by 7 circular zones, namely from closest to the pupil (1) stomach, (2) bowel (small intestine and colon), (3) heart, throat, pancreas, adrenal glands, proliferation, pituitary and pineal, (4) prostate, uterine and skeletal bones, (5) brain, lungs, liver, spleen, kidney and thyroid gland, (6) muscle, motor nerve, lymph and circulatory, and (7) sensory skin and nerves [8]

The iris chart is a division of the surface of the iris into several parts, and consists of 166 (80 right and 86 left) named segments and each part is associated with an internal organ or system in the body. The places of these organs are a reflection of each other in the right and left iris [3] and there are arranged in a shape resembling a clock face [9] and the iris divided into degrees clockwise [3] as in Figure 2a and Figure 2b.

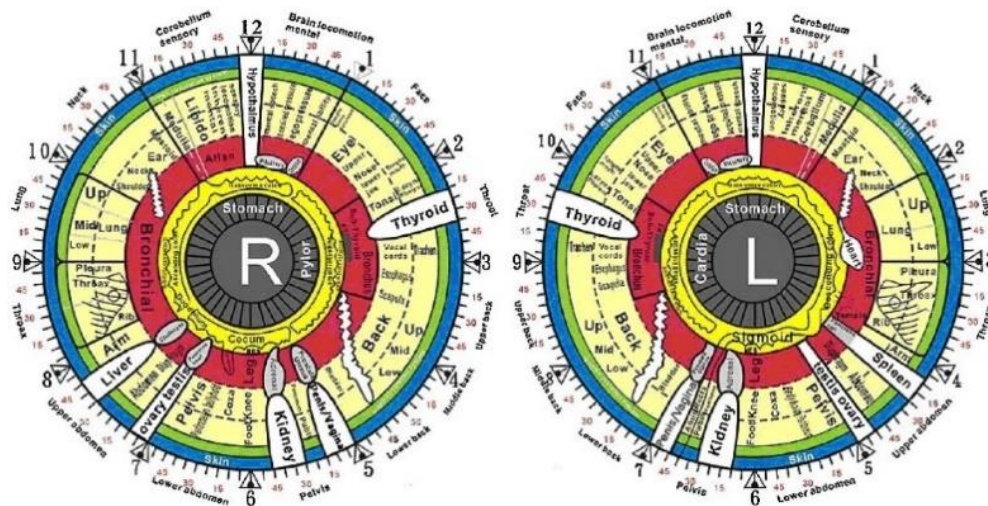


Figure 2a. The iris chart model (Right and Left iris) [10]

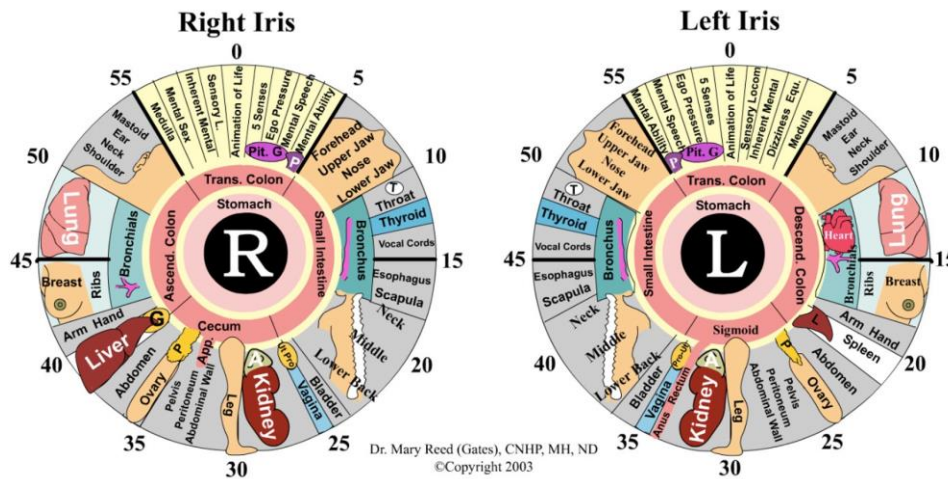


Figure 2b. The iris chart model (Right and Left iris) [8]

Also, German Iridology studied another form of iris chart represent the sign of diabetes in the Cross of Andreas in the iris. The Cross of Andreas can be seen in the two eyes as four holes (fiber openings) situated at 10, 20, 40 and 50 minutes, contrasting the iris and the clock [11].

Besides what was mentioned above, the science of Iridology has an active role in the treatment of traditional Chinese medicine (TCM). TCM practitioners classify the body's working system into 5 organs, namely heart, liver, kidneys, stomach (including spleen), and lung, which are related to the five elements of the universe, namely fire, wood, water, earth, and metals, respectively, based on morphological and functional similarity [12].

The concept of Iridology is focused on the integrity of tissues if the integrity of distant organs in the body is inferred by the structure, color and density of the microfibrils of the iris and is called "Tissue Integrity". Tissues are affected by changes in blood circulation, blood pressure, toxic settlements, inherent weakness, metabolic disorders and the amount of oxygen in the blood. Therefore, the analysis of the iris depends on the assessment of the stages of tissue integrity, so there are four stages of tissue activity named acute, subacute, chronic and degenerative, as in Figure 3 and they are indicators of the metabolism and metabolism of these cells [9].

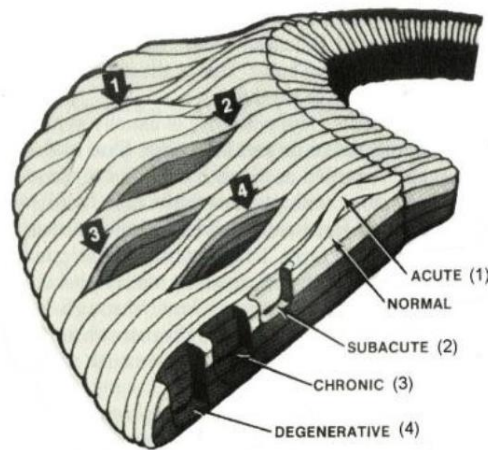


Figure 3. The cross-section view of iris image with the four stages of iris tissue [9]

In this study, the research related to the diagnosis of diseases by Iridology is reviewed by building diagnostic systems based on computer vision, image processing methods and artificial intelligence from 2009 to 2024 and indicating the methods, results and conclusions of these systems.

## II. OVERVIEW OF REVIEW PAPER

Research that is concerned with the development of disease detection systems by iris is ongoing now; over the past 15 years, researchers have worked on many researches, including below and as listed in Table 1, Which shows the working approach of each research and indicates the accuracy of the classification that was reached and the tool that was used to build each system.

R. A. Ramlee et al., [4] used iris recognition methods to detect high cholesterol in the blood, using Daugman's rubber sheet model, Hough transform to detect the iris, and Otsu threshold value with Histogram plot to distinguish the presence of a sodium ring in the iris. If the threshold value is greater than 139, the presence of high cholesterol is detected, but if the threshold is lower than that, the eyes are normal and the person is healthy.

Z. Othman et al., [3] proposed a new approach of iris segmentation to obtain a better and more accurate iris image called the water flow method for use in the fields of biometrics and Iridology.

C.-L. Lai et al., [7] used Fuzzy k-Ellipses (FKE) theory to reflect the severity of the disease, using the threshold morphological process and applying Sobel operations to detect the edge of the pupil location. Finally, a 2-D Gabor filter was used to extract image features.

Sivasankar K. et al., [9] proposed a system that consists of four stages, which are the acquisition of images for taking pictures, the pretreatment of the selected boundaries using the circular Hough transform, as well as using the means of Fuzzy C-Means and (gray-level analysis and Iris marker analysis) for analysis the iris. Finally, the system is effective, with a total accuracy of 84.38%.

S. E. Hussein et al., [10] used artificial intelligence technology by using an Adaptive Neuro-Fuzzy Inference system (ANFIS) based on Surgeno-type fuzzy and 2-D Gabor to analyse the image and detect the problem in the kidney. The adopted protocol separates the iris from the pupil and the sclera after converting the image to the gray levels, and then it is converted to polar coordinates using the Rubber sheet model. The results are encouraging, with an accuracy of 93% for the healthy group and 82% for the kidney problems group.

D. H. Hareva et al., [13] designed an iris application to diagnose the heart, lung, spleen and liver using Canny edge detection, Gaussian filter and Sobel detection. The objective of this work to detect and separate the iris as well as the pupil from the image. Also, an artificial neural network (ANN) type Back-propagation Neural Network was used to classify the disease. ANN consists of three layers. The weights of 11 features represent the nodes of the input layer, one hidden layer consisting of 4 nodes representing the 4 diseases, and one node in output. The diagnosis decision based on comparing the ROI for each disease. Finally the method works well with an accuracy of 90%.

S. P. Jogi et al., [1] studied the effect of iris image processing and various parameters of the algorithms used to design diagnostic systems based on Iridology. In addition to the duration required to capture those images and their quality and resolution to detect the iris' features, the system relies on obtaining images using Near infra-red sources to reduce reflection. Where the images are converted to the gray level and from 8 bits to double the resolution. The time required for the localization step is the longest, so the image size must be changed to control this time. Hence to controlling the localization speed and thus system speed.

A. Bansal et al., [14] proposed a system for diagnosing diabetes type II based on Iridology. The 2-D wavelet tree technique was used to extract the features from the dataset images of the eyes of 80 people, 40 of whom had healthy irises and 40 of whom had unhealthy irises. The machine learning technique type support vector machine (SVM) was used in the classification where the dataset was divided into 4 random totals, 1 part was used for testing and 3 parts for training the classifier. The highest accuracy, 87.5% was obtained using RBF kernel function.

M. A. R. Sitorus et al., [15] proposed a system for detecting chronic renal failure (CRF) stage 5 based on iris. Iris camera type Dino-Lite took images of the right and left irises of 40 patients in the hemodialysis stage. The iris features were extracted using the watershed technique, and the Sobel filter from the Region of Interest (RIO) for the kidney was used. The system accuracy (90%) for the right Iris and (94%) for the left iris. It was noted that the patient who had previously removed one of his kidneys did not show any abnormalities in the iris tissue corresponding to side that removed the kidney.

K. E. Martiana et al., [16] This proposal was characterized by using an automatic cutting method for the iris and the RIO that can produce three cutting results were success, scarce, and fail, using a threshold algorithm based on the threshold value taken from the average histogram learning data and the binary method of converting the image to bicolor to complete the cutting process, a series of image processing was used, including a Sobel filter, a median filter and the process of splitting, feature extraction and classification. The system was tested using images eyes of 40 normal and abnormal patients with an accuracy of 86.4%.

R. Agarwal et al., [17] proposed a system aimed at verifying Iridology in the diagnosis of diabetes. The principle of the system based on cutting the ROI for the pancreas in the iris area from the rubber sheet model and extracting the 63 features of them using means of two-dimensional discrete wavelet transformations (DWT), and circular Hough transformations (CHT) to extract the internal and external coordinates of the iris. Six different methods of machine learning were used in the classification process for the data of 100 people have diabetes and 100 people was healthy. The best accuracy was 89.66% with RF classifier.

P. Samant et al., [18] proposed a system to diagnose type 2 diabetes using machine learning. Six different classifiers and different feature algorithms were used to investigate and compute the best suitable algorithm and classifier according to the dataset. Depending upon the scoring criterion of each feature selection method, 10 to 50 top-ranked features were selected, and the best classification accuracies have been calculated by t-test feature selection method as 89.63%, 89.38% for 40 features and 89.97%, 89.18% for 50 features by Random Forest (RF) and Adaptive Boosting Model (AB) classifiers respectively by using the total data of 338 subjects (180 diabetic and 158 non-diabetic).

P. Moradi et al., [19] worked to verify Iridology of the prediction of diabetes mellitus by using the active contour algorithm, Histogram equalization and down sampling, Rubber sheet model and Gabor Filter, Histogram of Oriented Gradients (HOG) and Local Binary Pattern (LBP) to extract features. And 5 models of machine learning classifiers model to classify diabetes for 106 eye images with diabetes and 124 were healthy, so this was done by designing two experiments. The first was to verify the Andreas cross method, and the results showed the best classification accuracy of 91.8% with AdaBoost classifier and settings (pixels, HOG, LBP and Gabor filter) to extract the features. The second experiment to identify more useful distinctive areas in the iris to determine diabetes using 20% of the data to investigate based on the best model from the first experiment, the method produced 4 updated areas close to the

areas of the Andreas cross can be used as a new marker of diabetes due to the improvement from the first experiment with an average accuracy about 0.6% which leads the diagnosis more accurate than one area.

T. Hussain et al., [5] designed iris-based Lung pre-diagnosis system (ILPS) using an artificial intelligence algorithm. Gabor features-based blob detector was used, which extracts features based on the difference in color patterns and contrast in iris segments, and used a machine learning algorithm, type SVM, to classify a dataset of 100 eye images for lung diseases and 100 for good health. The system worked in a real-time environment and was tested by 50 eye images of people suffering from lung diseases. The result of the classification accuracy of the system was 88%.

P. Samant et al., [20] designed a diagnosis diabetes system based on iris features and machine learning independent on segmentation of the iris using the CHT and RIO representing the pancreas after normalizing the rubber sheet. The total number of features was 113, 31 features for each of the three RIO for the pancreas were extracted to determine and detect the condition of the iris tissues divided in to statistical features, including average density, contrast, correlation, standard deviation and entropy, and textural features including Gray-level co-occurrence (GLCM) and Gray-level run length (GLRL) matrix, in addition, 20 physiological features. And 9 different types of supervised machine learning classifiers to classify 250 people with diabetes and 84 healthy. The best accuracy was 95.81% with modified t-test and EBoT classifier model.

C. Banowati et al., [2] they proposed Android application to detect cholesterol levels in the human body based on iris, by taking pictures of the eye through the mobile camera. The design depends on CNN method in deep learning to classify the image and get the best model and condition of this method using a pre-trained model of Inception-v3 on a set of 90 images. The result was the best performance with an accuracy of 97.45% when the Epoch value was 800, batch size 100, and learning rate values 0.01.

A. Bansal et al., [6] developed an automated pre-diagnostic system to help doctors, aimed to predict obstructive pulmonary disease (OLD) and not diagnose it by using a database consisting of 49 eye images for people with obstructive pulmonary disease and 51 for other healthy people. The system combined the iris recognition system based on a two-dimensional Gabor filter to extract features, and SVM machine learning system to classify the disease, as well as pre-processing of the iris in which the CHT to localize the iris and the Daughman's rubber sheet model to normalize the iris image, in addition used histogram and threshold analysis. The system achieved an overall accuracy of 88% using the RBF kernel function.

P. A. Reshma et al., [21] proposed a system to detect heart abnormalities and high cholesterol in the blood. Training the system by inserting eye images to the pre-processing step, which includes a medium filter to remove noise, a segmentation process to crop the image by histogram, convert the image to black and white to obtain a binary image, and the second step to extract features by calculating the ratio of the number of white and black pixels, and then the classification process by determining the threshold value. The process of determining high cholesterol is carried out by localization process by using the method of an integro-differential operator (IDO). Through this research, it was found that high cholesterol and heart abnormalities are closely related.

Y.-H. Li et al., [12] proposed a real-time system application that assesses the health status of the human body based on Iridology and Chinese alternative medicine (CAM) with the predictions of expert opinions from the Taiwan International Institute of Iridology (TIII) to classify the human body into 9 categories by using deep learning (DL) concept. First, the system obtained the iris images and applied image processing by using contrast limited adaptive histogram equalization (CLAHE) to enhance the contrast and division of the iris. And then, Segmentation iris uses the R-CNN (Regions with CNN features) model to detect and classify the position of the eye in the image, as well as the Gaussian mixture model (GMM) to find the pupillary area. A conventional neural network (CNN) with three models was used to classify images, each of which was trained with a transfer learning technique. The best accuracy was 82.9% with the Dense Net 201 model.

L. B. Rachman et al., [22] proposed a system for detecting cholesterol levels by analyzing iris patterns. In this system, the first stage was to obtain images from the UBIRIS database, where 10 eye images were obtained were for people with high cholesterol and 20 for people without high cholesterol. The second stage was image pre-processing, including converting the color image to grayscale, Median filter, then converting the circular iris image to a rectangular shape, and then allocating the ROI for the cholesterol ring, then the image filtered by Gaussian filter to obtain a smooth results. Features were extracted from the iris using GLCM. The third stage was classification by using a back-propagation neural network. As a result, the accuracy rate was 96.67%.

L. B. Rachman et al., [8] they proposed a system for detecting upper stomach disorders. The image preprocessing was done by cropping and changing the image size to improve the image quality and convert the color image to a gray image. The classification process used Back propagation artificial neural networks trained by iris images containing 10 pairs for people with upper stomach disorder and 10 pairs for healthy people. The system accuracy was 55%.

S. Muzamil et al., [23] developed Intelligent Iris-based Chronic Kidney Identification System (ICKIS) using artificial intelligence and Iridology. The system principle by applying the deep learning type CNN model to extract features from the ROI and classify the image, where the artificial intelligence algorithm trained and tested on a GPU-based supercomputing machine by using dataset include 2000 eye photos of healthy people and 2000 photos of people with chronic kidney problems. In addition, the preprocessing stage was used for iris images, where the supercomputer provides a high peak processing performance. The system achieved diagnostic accuracy for detecting kidney disease with 96.8 %.

C. Yohannes et al., [24] designed a heart disease detection system using computer vision, machine learning and Iridology. The dataset contains 55 eye images for people with heart disease and 55 for healthy people. 88% of this data was used for training and 22% for testing. The system contains two stages, the first stage was processing using a pre-processing process, which includes converting the RGB image to gradient Gray, increasing the contrast between the iris and its surroundings by using CLAHE, smoothing the image by using a medium filter, then circular Iris was converted to linear to extract the ROI which was resized to extract the important features by using Canny edge and Principal Component Analysis (PCA). The second stage was the classification and prediction of the disease by using a Back-propagation Artificial Neural Network algorithm. The accuracy was 95.45%, with best values of Sigma 0.3 for canny edge detection, 50 PCA, 50 hidden neurons and 0.01 for error limits.

H. A. U. Rehman et al., [25] the proposed application for iris-based kidney disease detection system and deep learning. The design of the system by CNN with 5 layers, three layers was convolution and two layers was dense layers. Rectified Linear Unit (ReLU) activation function used for the first 4 layers, and soft-max activation used for the last layer of the network trained by using 49 eye images of people with chronic kidney disease. The system diagnostic accuracy was 86.9%.

E. M. Kusumaningtyas et al., [26] they proposed a desktop application for an iris-based diabetes and heart disease detection system that could be used in a healthcare kiosk. The system consists of a pre-process stage that includes median filter, color detection and auto-cropping using integral projection to remove the sclera, and then finding the ROI for heart and pancreas to extract features. The last stage was classification process that used threshold method which worked by calculating the average ratio of black and white from the training dataset that consist of 31 images to find the threshold for normal and abnormal eye. The system accuracy was 83.87 % for diabetes and 80.65 % for heart disease.

S. K. Punia et al., [27] proposed a system in the form of a desktop application that can be used in a healthcare kiosk to detect diabetes and heart disease based on Iridology. The system consists of 5 stages, the first stage is obtaining data. The next consists of real-time processing, which includes segmentation and normalization. Preprocessing, which includes cropping the image, color detection and medium filter. Extracted the ROI for heart and pancreas from the left iris. Next was a classification that used the threshold method: the average composition of the black and white training dataset of 32 images. The last stage was the outcome decision, which determined whether the result was abnormal or normal. The accuracy was 90.91% for diabetes and 86.36% for heart disease.

F. Özbilgin et al., [28] they proposed an iris-based coronary artery disease (CAD) prediction system by machine learning. The system contains 94 eye images with CAD and 104 without CAD. The first stage of designing the system was the pre-processing stage, which include converting the color image to grayscale, localization using the IDO, normalization using Daugman's rubber sheet, then cropping the RIO, then increasing the contrast of ROI by CLAHE method. The next was features extraction using Wavelet Transform, First-Order statistical analysis by GLCM and Gray Level Run Length Matrix (GLRLM), Relieff feature selection process was used to determine the top features before classification. And the last stage was classification process by using 22 classifiers from five main families. The best accuracy rate was 93% to predict CAD with SVM.

S. J. Wagh et al., [29] they suggested an Android application for detecting heart diseases using Iridology. The system consists of many stages, the first stage was pre-processing that contains median filter and high-pass filter to improve image quality, automatic iris cropping process by using histogram analysis, and Sobel edge detection to extract Iris lines to obtain a clear iris image. Then, segmentation the iris to obtain the ROI and it converted to binary image to extract important features. After that, calculate the average ratio of black and white pixels from the training dataset consisting of 30 eye images to obtain the threshold value used to classify the data to normal or abnormal. Android system achieved 95.78% accuracy of diagnosis of heart disease.

C. Fernandez-Grandon et al., [30] they proposed a new approach to diabetes detection based on Iridology and machine learning. The dataset obtained from images of both eyes of 106 people with diabetes and 124 healthy. The system processes convert the RGB image to grayscale, cropping the image to include the iris, changing its size to reduce calculations and converted to one-dimensional matrix, changing the brightness and contrast and then applying geometric transformations to increase the number of images to 1300 images. Then reduce the size of the matrix components by selecting 10% of the pixels selected by chi-square and selecting 13 features from the PCA that used to feed the disease classification part as the inputs to Extreme Learning Machine (ELM) algorithm with Adam

(Adaptive Moment) optimization that hidden layer contains 256 neurons, learning rate of 0.01, batch size of 128 by using ReLU activation function. After a five-fold validation, the system worked with integrated performance and an average accuracy of 99.92%.

Table 1: Summary of systems that mentioned in this review paper (see APPENDIX).

No.	Year	Ref.	Processing and Features Method	Classification Method	Model	Data Type	Tool Type	Diseases Type	Accuracy %
1	2009	[4]	HT + Daugman's rubber sheet	Histogram + Otsu's threshold	Thr.	UBIRIS	MATLAB	High cholesterol	-
2	2010	[3]	Water flow method	-	-	-	-	-	-
3	2010	[7]	2-D Gabor filter + Morphological features + Sobel edge detection gradient + CHT	FKE	ML	-	-	-	-
4	2012	[9]	-	Fuzzy C-Means	ML	Web	IDL V.6.3	Lung	84.38%
5	2013	[10]	Wavelet (2-D Gabor) + Discrete 2-D Gabor Transform + CHT	ANFIS	ML	-	-	kidney	93% with normal and 82% with kidney
6	2013	[13]	Canny Edge Detection + Gaussian filter + Sobel operator	ANN	ML	Electronic books or on internet	Java + C#	Heart + Lung + Spleen + Liver	Heart 95%, Lung 90%, Spleen 90, Liver 90 %
7	2014	[1]	IDO + Gaussian smoothing function + Daugman's rubber sheet	-	-	CASIA V.1.0 + UBIRIS + UPOL + Image taken	MATLAB	-	-
8	2015	[14]	CHT + Homogeneous rubber sheet + 2-D Gabor filter + 2-D DWT	SVM	ML	-	MATLAB	Diabetes	87.5%
9	2015	[15]	Watershed Transform + Sobel filter + ROI	-	-	Image taken	-	kidney	90% for right and 94% for left iris
10	2016	[16]	Iris Cropping + Sobel operator + Median Filter + Binarization + Histogram	Threshold	Thr.	Mugi Barokah Clinic	C#	Heart	86.4%
11	2017	[17]	Iris Cropping + Rubber sheet + DWT+ CHT	BT, RF, AB or AdaBoost SVM, GL, NN	ML	Image taken	-	Diabetes	89.66% The best for RF
12	2018	[18]	Iris Cropping + Rubber sheet + DWT + CHT + GLCM	BT, SVM, AdaBoost, GL, NN, RF	ML	Image taken	-	Diabetes	The best for RF 89.63% for 40 features and 89.97% for 50 features
13	2018	[19]	Active contour + Rubber sheet + Histogram equalization and Down sampling + Gabor Filter, HOG and LBP	SVM, AdaBoost, NN, RF, LDA with shrinkage parameter.	ML	Farabi Eye Hospital	-	Diabetes	91.8% Andreas cross with the best for AdaBoost and 92.4% for New 4 area
14	2019	[5]	Gabor features	SVM	ML	Image taken	CAFFE	Lung	88%
15	2019	[20]	CHT + Rubber sheet + Iris Cropping + GLCM + GLRL + modified t-test and PCA filter	CT, MT, QSVM, CSVM, FGSVM, MGSV, EBoT, EBaT, SKNN	ML	Image taken	MATLAB	Diabetes	95.81% The best with modified t-test and EBoT
16	2019	[2]	-	CNN with Inception-v3 model	DL	Image taken	MATLAB + Tensorflow	High cholesterol	97.45%
17	2019	[6]	2D Gabor filter + CHT +	SVM with RBF kernel function +	ML +	Image taken	MATLAB	Lung	88%

			Daughman's rubber sheet	Histogram + Threshold	Thr.				
18	2019	[21]	IDO + Median filter	Histogram + Threshold	Thr.	Image taken	-	High cholesterol + Heart	-
19	2020	[12]	CLAHE + GMM	CNN (Inception V3, ResNet, DenseNe)	DL	CASIA-Iris-Thousand database	MATLAB + Python + Tensorflo + KERAS	Lung + Kidney + Liver + Heart + Spleen+ Stomach	82.9%
20	2020	[22]	GLCM + Gaussian Filter + Median Filter	Back-propagation Neural Network.	ML	UBIRIS	-	High cholesterol	96.67%
21	2020	[8]	-	Back-propagation Artificial Neural Network + MSE	ML	Image taken	MATLAB + CVIPtool + PhotoScape	Stomach	55%
22	2020	[23]	Pre-processing	CNN	DL	IIMCT-Pakistan	OpenCV + Python + Tensorflow	kidney	96.8%
23	2020	[24]	CLAHE + Canny edge detection + PCA + WarpPolar function	Back-propagation Neural Network	ML	health care center	-	Heart	95.45%
24	2021	[25]	-	CNN	DL	Image taken + Bahawal Victoria Hos.	KERAS	kidney	86.9%
25	2021	[26]	-	Threshold	Thr.	Image taken	Kiosk	Heart + Diabetes	83.87% for Diabetes and 80.65% for heart
26	2023	[27]	Cluster analysis	Threshold	Thr.	Image taken	Kiosk	Heart + Diabetes	90.91% for Diabetes and 86.36% for heart
27	2023	[28]	wavelet transform + GLCM + GLRLM	SVM, DT, NB, KNN, NN	ML	Giresun Uni.	MATLAB	Heart	93% SVM the best
28	2023	[29]	Cropping image + Histogram analysis + Sobel edge	Threshold	Thr.	Image taken	Java	Heart	95.78%
29	2023	[30]	Chi-square + PCA	ELM + Adam + ReLU activation function	ML	Image taken	Python	Diabetes	99.92%

### III. METHODOLOGY (MATERIALS AND METHODS)

By reviewing the systems used in the research papers in this review paper, the main structure of the iris-based disease diagnosis system consists of 6 main stages in general, namely dataset acquisition, processing the eye images, region of interest (ROI), features extraction, classification the dataset and diagnosis results as shown in Figure 4.

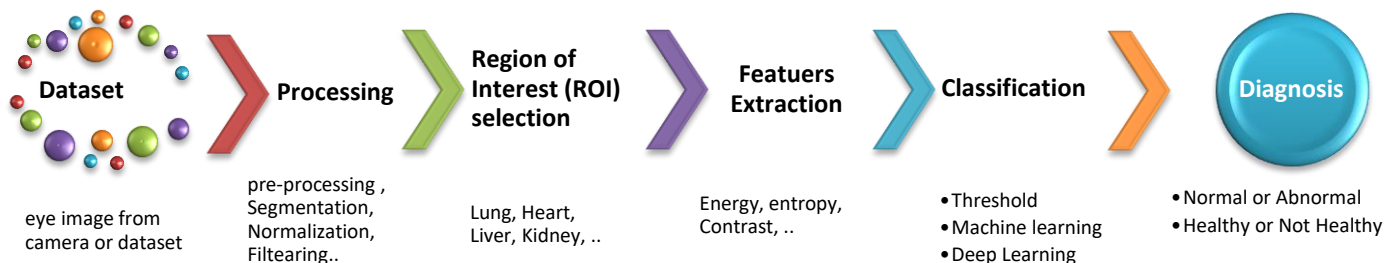


Figure 4. General Diagnosis System Model

The design and implementation of the construction of the diagnostic system on computers or smartphones is carried out according to the principle of computer vision, image processing, and artificial intelligence tools using one of the software tools and programming languages. In the researches that has been reviewed used MATLAB software, OpenCV computer vision, IDL (Interactive Data Language) version 6.3, C# language, Java language, python language with Tensorflow, KERAS and CAFFE Framework, as well as in

some method added auxiliary tools for image processing CVIP tool and PhotoScape. According to Table 1 MATLAB program is used in the most diagnosis systems designs as shown in Figure 5. The MATLAB program can process iris images and detect organ disorders with accuracy, speed and high efficiency [22]. These stages and all parameters can be described in the following paragraphs.

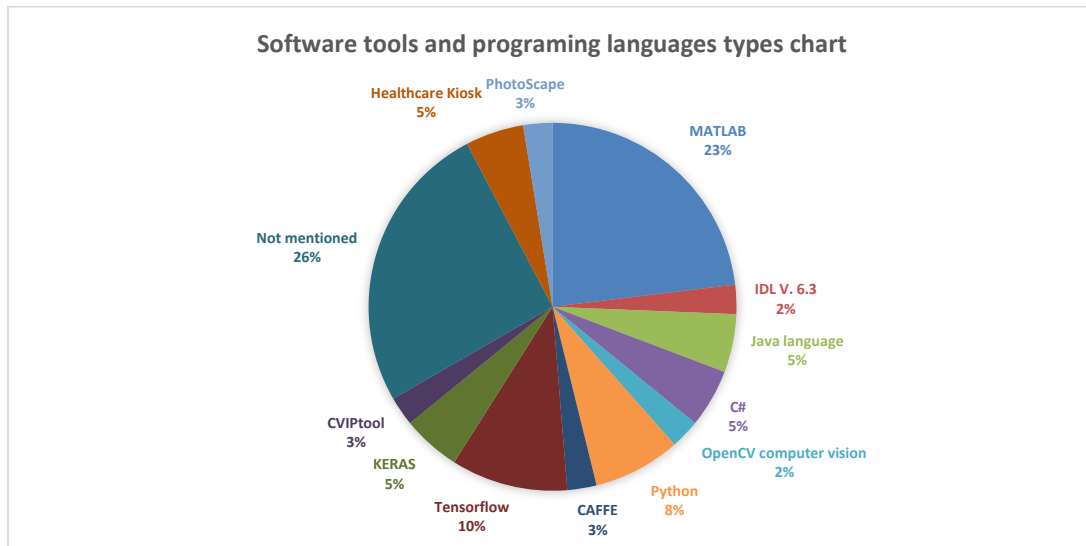


Figure 5. The chart of percentage the software tools and programming languages that used in researches according to Table 1

#### A. Dataset Acquisition Stage

Inputs data to the detecting diseases system based on iris are images dataset or eye images captured from camera [4]. In Table 1 list of the types of datasets mentioned in these review papers. Figure 6 represents the dataset chart according to this table, and it turns out that the most used datasets in these detection systems take direct images of people's eyes. The classifier operates at the best case, using thirty percent of the data for testing and seventy percent for training the classifier [17].

When taking eye pictures, it is necessary to pay attention to special limitations that ensure the efficiency of the diagnostic system. So, to get the best image of the iris, the center of the iris and pupil should be at the central point of the camera used and the location of the eye is straight while taking the image [27] and the best distance to take an eye image is 5 cm at an angle of 0° and the luminous intensity is 150-300 Lux [2].

To obtain more accurate features of the iris from the eye image, a camera with high resolution, high specifications and additional flash lighting are used [21].

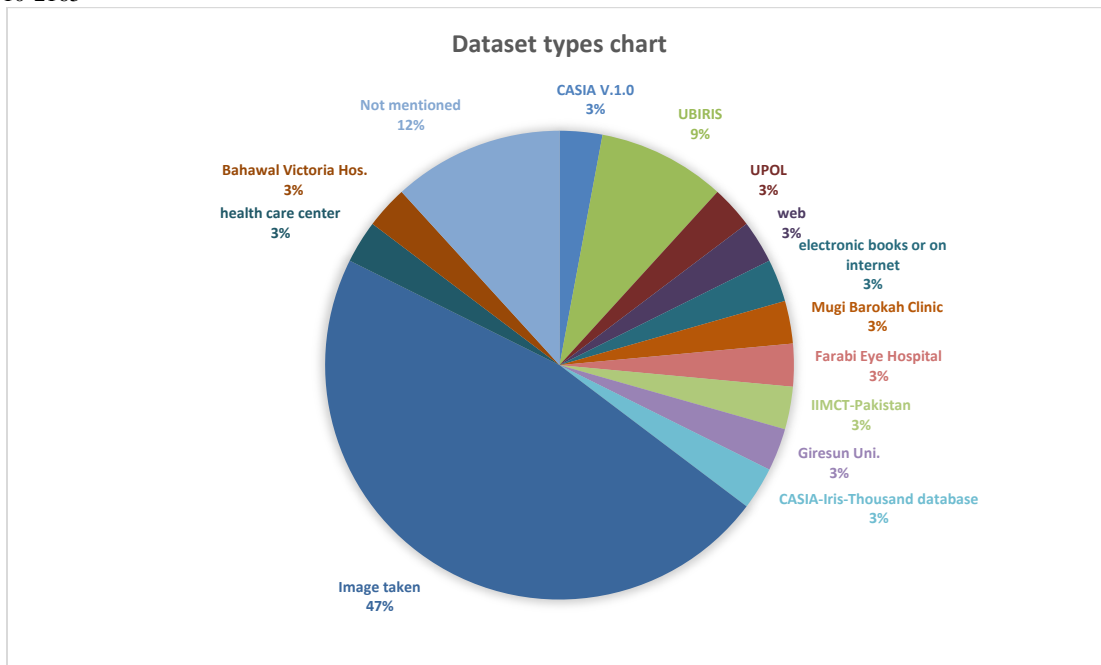


Figure 6. The chart of dataset types that used in researches according to Table 1

### B. Processing Stage

The design of iris diagnostic systems often includes a number of steps of image processing, which may include some of the stages indicated in Table 2. Where the pre-processing step converts color images to gray to simplify operations. Localization of pupil and iris step has the task of detecting the circle of the iris circumference and the circle of the pupil, and measuring the center of the iris and pupil in the coordinate system [3]. In general iris localization is used to locate the inner and outer boundaries of an iris [10]. Also, it is usually preferred that the diagnostic images of the iris are isolated from the eyelids and eyelashes [3]. Segmentation step is the process of segmenting the iris area of the eye image and is important for the completion of the normalization process [1] [20] as in as in Figure 7 [10]. The normalization step task is the transformation the iris of the eye from a circular shape to a rectangular shape as in Figure 8 [4]. This step is important for the diagnostic system in order to record the images and compare them with the iridology chart [1]. As for the filtration step, it removes noise and get the best results [13] [16]. Figure 9 represents the diagram of the implementation the image processing stage (all images in the diagram selected from different papers in this review [30], [10], [18]).

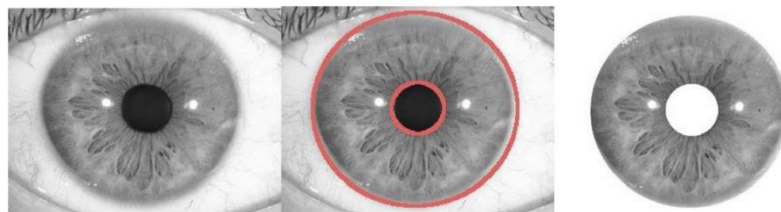


Figure 7. Stages of iris localization. Left, grayscale eye image. In the middle, two circles are overlaid in red for iris and pupil boundaries. Right, the segmented iris. [10]

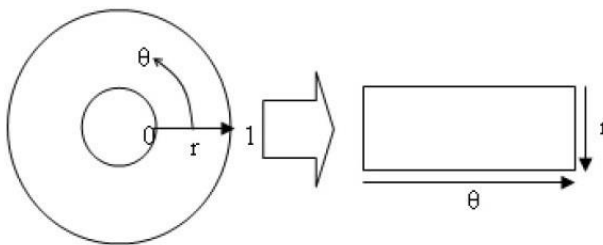


Figure 8. Daugman's rubber sheet model [4] , or transformation of the iris from Cartesian coordinates to polar coordinates [10].

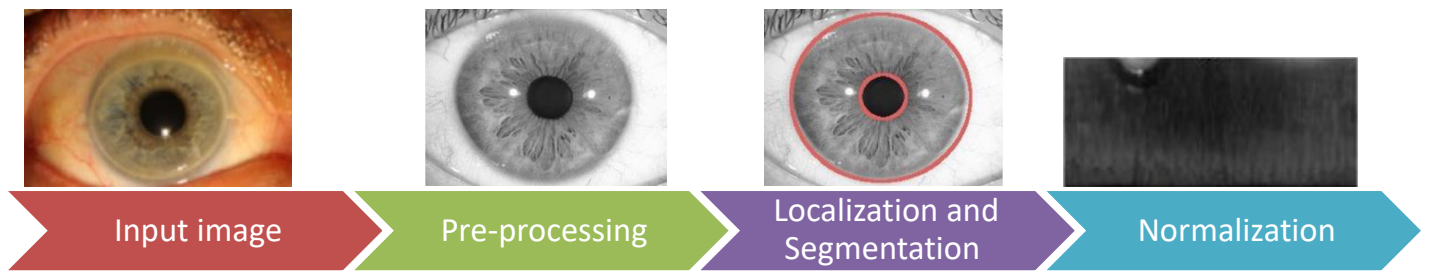


Figure 9. The diagram of implementation the image processing stage.

Table 2. Summary of processing stage in systems that mentioned in this review paper.

Processing stage types	Methods	summary
Pre-processing	Image Manipulation	Transformation the images from RGB to gray level and from eight-bit to double precision thus simplify the manipulation of the image [1].
	Binarization Image	It is a black and white image with a color value of 0 and 1 [16].
	Gray level analysis or Grayscale	Convert the RGB to grayscale to simplify processing operations [22]. Normalized gray level making the image have a gray level of 0 to 250 [13]. This method useful to extract features from images according to the intensity value of the four stages of iridocyclitis activity to identify problems, the gray levels are represented, White for acute, light gray for subacute, dark gray for chronic and black for destructive or terminal stages of the disease [9]
	Binary Method	It converts the RGB image to a binary image to collect the values of the weights of black and white pixels that used in extracting image features [16].
	Contrast Limited Adaptive Histogram Equalization (CLAHE)	It is one of Histogram equalization method that used in pre-processing step to increase the contrast between the iris background and the iris fiber feature [24].
Localization and Segmentation	Circular Hough Transform (CHT)	Used to detect the edge of the pupil circle and the edge of the iris [4].
	Sobel Operation	To detect the edges and used because it provides differential values and characterized by a smoothing effect, and it consists of gradient operations, one horizontal and the other vertical [7] thus used to find the magnitude and direction of the gradient [13].
	Canny edge detection	To detect edges or contours of shapes in the image [13].
	Integro-Differential Operator (IDO)	Used by Daugman to find the arches of the upper and lower eyelids, and to determining the pupil area and the circular Iris [1], The iris's boundaries are accurately identified using the IDO method [21]. In order to achieve accurate localization, the operator application is repeated while reducing the amount of smoothing, and in order to increase the localization speed and reduce the diagnostic time, the image size is reduced, but with a limited range, because this reduces the localization accuracy [1].
	Water Flow Method	It is used to divide the iris of the eye and provides high geometric flexibility and adaptable topology, using physical measurement instead of other more complex methods. It is very useful in medical imaging, because of the complexity of its images [3]
	Watershed Method	It is one of the powerful methods to produce an initial image segmentation. To extract the gradient information, a Sobel filter is used and then it is entered into the watershed transformations. the gradient values from the initial segmentation image are benefit for calculating the edge strength values [15].
	Thresholding	It is one of the important methods used to Segmentation the image, as it is used to separate the pupil, Iris and sclera by extracting pixels from the background by determining the threshold value to separate the part [7].
	Active Contour Model	It is utilized to detect the outer boundaries of the pupil and iris. And it is more stable and accurate than the Hough transform for iridology purposes [19].
Normalization	Daugman's rubber sheet model	The image size is changed to fit the size of the iris map by transform the iris image from Cartesian coordinates to polar coordinates[10], as shown in Figure 8
	Warp Polar function	Converts the circular image of the iris into a linear shape as a rectangle image [24].
Opening	Erosion, Dilation, Opening and Closing	Used to eliminate noise in the morphological processes of image processing by simplifying the shape of the object to get rid of background noise or to enhance the structure of the image as the structure of the object such as thinning and thickening [7].
Filters	Gaussian Filter	The benefit to reduce noise in photos so that they look smoother [13].
	Median Filter	It is used to smooth and remove noise from the eye images[16]. For removing outliers without compromising image sharpness, the median filter is superior [21].
	High Pass Filter and Low Pass Filter	The sum of these two filters is used to sharpen the image to improve image quality and get the best results [16].
	Fisher score discriminator, t-test and chi-square test	Three famous filters based on the feature selection method. The feature is selection with medical applications based on computational efficiency and popular simplicity in this field [18].

C. Region of Interest (ROI) selection stage

After the image is pre-processed, the ROI is selected. The goal of this stage is to crop the area containing the organ [20] to be diagnosed by the system to extract features from it to identify the condition of the organ [24]. Where the ROI [9] means the location of the area containing the organ in the iris chart, mapping the ROI iris using a circular area is represented by the angular size 0° to 360° or analog clocks from 0 to 12 o'clock, each 30° is equal to 1 o'clock [13]. In Table 3 clarifies the signs and locations at the iris chart of some organs that are related with diseases diagnosis based on iris mentioned in this review paper as in Figure 2a and Figure 2b above, as well as in Figure 10 many examples for ROI that shows the marks and pattern of kidney in both eyes [23]. Figure 11 represents the diseases chart according to Table 1 above and it turns out that the most commonly treated diseases is diabetes and heart.



Figure 10. ROI Marks and patterns showing kidney problems (a) Right eyes (b) Left eyes [23].

Table 3. Summary of ROI in systems that mentioned in this review paper.

Organ or Disease type	ROI and signs summary
High cholesterol	Indications of high cholesterol or Hypercholesterolemia in blood are the presence of a gray or white ring around the iris of the patient's eye [4]
Lung	ROI for the lung in the iris chart is located at in 9 to 10 o'clock regions for right iris, and 2 to 3 o'clock regions for left iris [9]. The lung problem contains four stages of Iris tissue activity, namely acute changes, subacute changes, chronic changes and degenerative changes [9]. In the event of disorders or dysfunction of the lung signs appear in the left or right part of the iris of the lung and according to the location of the relevant lung in the form of spots such as white clouds or mucus can be seen in the form of white clouds around the outer part of the iris [5].
Kidney (Chronic Renal Failure)	ROI of kidney disease is set at 5.35 to 5.95 o'clock for right eye and at 6.05 to 6.6 o'clock for left eye, on the third quarter of the circle for right eye and on fourth quarter for the left eye [15], any change in kidney appear at the bottom edge of the iris [23].
Liver	ROI of liver on angles ranges from 235° to 242° in the right iris [13].
Spleen	ROI of spleen is set on angles range of 125° to 132° in the left iris [13].
Heart	ROI of heart is located between 2 to 3 o'clock of left iris [13].
Diabetes	Diabetes occurs in pancreas, the position of the pancreas head in the right eye between 7 to 8 o'clock and the position of the pancreas body and tail in the left eye in between 4 to 5 o'clock [14] Or position of the pancreas is placed in the second outer circle after the pupillary area at 03.50 - 04.20 in left eye [26]. Or Diabetes sign represented in cross of Andreas sign [19].
Stomach	Any change in the stomach can cause change above the pupil directly in the iris [12].

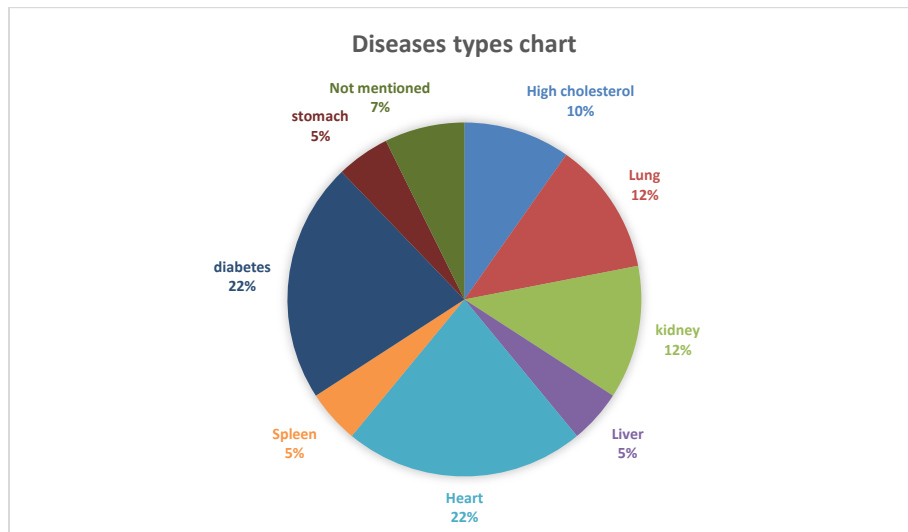


Figure 11. The chart of diseases types that used in researches according to Table 1

#### D. Feature extraction and selection stage

The most important stage after segmentation is feature extraction to measure the density of the iris image, the shape of the iris, the pupil, whether it is round or not, and the edge mark on the iris [3]. The statistical and textural features extracted from ROI are used to quantify the broken tissue information of the iris [17]; statistical features usefulness is to study the nature of gray pixels and provide information on the intensity of the gray level [20]. Also, feature selection strategies increase the reliability of categorization by eliminating redundant features [18]. To execute this stage uses some of the RIO features [17] and some of the feature types described [20] in Table 3, to form the matrix of features that are used in the subsequent training process to classify diseases.

Table 3. Features types summary

Feature types	Summary	Formula
Mean Intensity	- [17]	$\frac{1}{N} \sum_{i=1}^N X(i)$
Standard Deviation	- [17]	$\left(\frac{1}{(N-1)} \sum_{i=1}^N (X(i) - \bar{X})^2\right)^{1/2}$
Contrast	It is the difference between the highest and lowest values of a continuous set of pixels. And it shows the local variations in an image [20]. [17]	$\sum_{i,j}^{ i-j =1}  i - j ^2 P(i, j)$
correlation	measures its gray level linear relationship [20]. [17]	$\sum_{i,j} (i - \mu_i)(j - \mu_j) P(i, j)$
Homogeneity	-	$\sum_{i,j} \frac{P(i,j)}{1+ i-j }$
Variance	It is a measure of non-homogeneity in images [20]. [17]	
Energy	Measures an image's textural uniformity [20]. [17]	$\sum_{i,j} P(i, j)^2$
Entropy	Calculates an image's textural complexity [20]. [17]	$\sum_{i=1}^{N_i} P(i) \cdot \log_2 P(i)$
Gray-Level Co-occurrence Matrix (GLCM)	It is a second-order statistical method that calculates the frequency of pairs of pixels that have the same gray level [22]	-
Gray-Level Run Length (GLRL) matrix features	It is a matrix characterizing the distance of the gray level in various directions and represent the number of adjacent intensities of the same gray level [20]. This method used to extracting higher-order statistical texture features [28].	-
Histogram equalization	It is used to improve the contrast of the image. The contrast levels in the natural image are distributed uniformly and concentrated in the center of the gray level from 0 to 255. It requires calculating the density function, probability and cumulative density of the image to perform histogram equalization, in addition, it requires calculating the number of pixels for each color in the image and producing a running sum to count and thus make the histogram equalization. by scaling the output [10].	-
Histogram of Oriented Gradients (HOG)	One of the most common methods in feature extraction and texture detection that used to calculate the number of gradient directions in image areas [19].	-
Local Binary Pattern (LBP)	One of the most common methods in feature extraction and texture detection is based on comparing pixel values with their surroundings to calculate the normalized histogram of a binary image. Utilizing LBP and HOG together to achieve at improved results for classification purpose [19].	-
Down Sampling	For reducing redundancy in pixel information may be utilized additional down sampling as a feature selection method [19].	-
Modified t-test	It is a filter-based feature selection used to determines the significant difference between two classes by calculating the ratio of the mean difference and variability of the classes; however, it is restricted to two-class problems only [20].	-

Wavelet transforms	It is useful in many applications of wave transformation to texture analysis because it does not result in interfering terms as it is a linear process and has the ability to localize the time–space of the spectral features of the signal, unlike the Fourier method. Also, Wavelets can be used to analyze data that appear with different accuracy in the iris region into components. advantage of the Wavelets over the traditional Fourier transform in that the frequency data is localized, which allows matching features occurring in the same mode [10].	-
2-D Discrete Wavelet Transform (DWT)	It is used in non-stationary image analysis is highly advantageous[17] to perform the extraction of important features from the iris image, where it analyzes the original iris image of size $N \times N$ into 4 subsamples of images each of size $\frac{N}{2} \times \frac{N}{2}$ which are approximation (LL), horizontal (HL), vertical (LH), and diagonal (HH), and contains information from different frequency components [14].	-
3-Dimensional Wavelet Transform (3-D DWT)	It is used to compute the textural and statistical variables. decompositions display the high and low frequency image or ROI components. Using low pass (L) and high pass (H) filtering, image $X(l, j)$ is divided into 8 decompositions. Analyzing a digital image by splitting it down into its time and frequency components useful method for discovering concealed data. [17].	-
Gabor Filter	One of the most common methods in feature extraction and texture detection extracts frequency information in the region of interest in special orientations [19]. 2-D Gabor filter used in clinical applications to recognize alimentary canal disease and nerve system disease[14]. Where [7] : $(x, y)$ : coordinates of spatial region $\sigma$ : Gauss standard deviation function. $w$ : Frequency component $\theta$ : direction of filter parameters.	$g(x, y) = g'(x, y)e^{(j2\pi w\xi)}$ $g'(x, y) = \frac{1}{2\pi\sigma^2} e^{-\frac{x^2+y^2}{2\sigma^2}}$ $\zeta = x \cos \theta + y \sin \theta$
Principal Component Analysis (PCA) or Principal components (PC)	It is used to retrieve the most important features found in the data frame[24]. And it is a dimensionality reduction technique [30] whose filter-based feature selection represents a statistical tool that is the goal to uses orthogonal transformation to transform a set of highly correlated variables into linear uncorrelated variables [20]. [24]	$\text{Final Set} = \text{Features Vector}^T \times \text{Standardized Dataset}^T$

### E. Classification methods stage

After extracting features from ROI, the classification process is carried out to classify the types of disease to normal or abnormal and its stage, whether acute, subacute, or chronic, the system learning to determine the stage of the disease or its type [3] according to input image dataset that to be healthy or not healthy by using one or more of classification methods that based on a threshold or artificial intelligence types (ML and DL) as described some of them below:

#### 1. Threshold method

The famous method used in systems is the Otsu threshold method, which is a decision-making method when the algorithm assumes that the image contains two categories of pixels (such as foreground and background), then finds the best threshold boundary separating the two categories so that their common spread is minimal, i.e., the variation within the category is minimal [4]. Otsu’s threshold method is mostly used in clinical applications to detect the presence of cholesterol [14].

#### 2. Machine Learning Method (ML)

Machine learning is a branch of artificial intelligence (AI), which uses algorithms to teach machines and help systems learn [31]. This branch deals with the data patterns of many fields, including the field of medical diagnostics to improve the performance of its work, where the science of Statistics has evolved to provide statistical and computational theories basic to learning processes. The main types of machine learning methods include two types, supervised and unsupervised [32]. There are many Supervised machine learning methods that used in designing the classification stage or the overall diagnosis system. The famous methods are:

- Support Vector Machine (SVM): It is one of the modern machine learning methods proposed by Vapnik [14], and it is a well-liked classifier in the fields of text classification, voice recognition, image recognition, pattern recognition, and so on [6]. In addition, both Burges and Cristianini provided accurate information about SVM, where the hyperplane is formed to be the decision surface and the margin of separation between positive and negative is maximized in such a way. This machine learning technique is based on the principle of structural risk reduction. It is a binary classification that separates two categories in an ideal way[14] .
- Fuzzy theory: It is useful to determine the severity of the disease or the health status of patients. Also, it is used to calculate the data synchronously and consists of three steps, namely the input values, the point of specificity of the image features and the final result, which can contain a number of fuzzy functions to determine the severity of the disease [7] .
- Adaptive Neuro-Fuzzy Inference System (ANFIS): It is functionally based on the Sugeno-type fuzzy rule base and has an equivalent architecture at the same time allowing the system to learn from the training data. The design first started with subtractive clustering which is an unsupervised algorithm that relies on a measure of the density of natural data points in the feature space to determine the number of bases and input membership functions (such as the generalized Bell membership function that is suitable for detecting kidney disease) [10] .
- Artificial Neural Networks (ANN): The process of ANN is divided into two parts, learning and prediction, and consists of three layers. The analysis is based on the features of the iris texture. The process of predicting the health status of the organ is

carried out by evaluating the values of the results of the ANN in ROI. One of the types of ANN is a back-propagation neural network [13].

- Artificial Neural Network Back-propagation (ANN Back-propagation): It is one of the classification algorithms that is widely used in solving machine learning problems. The structure of the algorithm consists of a number of layers, including the input and output layer and the hidden layer, which consists of one or more layers, and each hidden layer can consist of more than two neurons as in Figure 12. The back-propagation algorithm consists of two stages, first is the training stage and the second is the testing stage. [24].

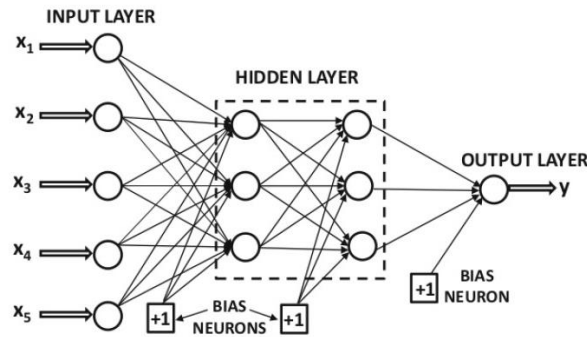


Figure 12. ANN Back-propagation Architecture [24].

- Extreme Learning Machine (ELM): It is a single-layer feedforward neural network (SLFN) learning algorithm where the parameters are set only once and do not need the iterative training. This algorithm is characterized by easy to implement, good performance and fast learning unlike traditional gradient-based learning algorithms such as back-propagation. Different algorithms can be used to improve the efficiency and adaptability of the ELM algorithm such as Adam algorithm [30].
- Adaptive Moment Estimation (Adam): It is an optimization and adaptive learning algorithm that automatically adjusts the learning rate based on the magnitude and direction of the gradients to improve efficiency, by combining the advantages of two optimization techniques, namely Stochastic Gradient Descent (SGD) and Root Mean Square Propagation (RMSprop). By taking advantage of the gradient information of the first and second order, the algorithm automatically assigns the learning rate to each parameter in the model and during the training process. The result is a faster and more stable convergence [30].

### 3. Deep Learning (DL)

Deep learning is one of the branches of artificial intelligence (AI) that focuses on building neural networks similar to the human brain and the nervous system, where it is characterized by its ability to perform complex tasks, technical knowledge, decision-making skills, having the ability to generalize and show intelligence and automation. Where it is considered a modern advanced step in machine learning, as it includes all the characteristics and advantages of ML. DL learns the relevant features from the data directly and does not learn manually as in ML. DL reduces the effort and time of operations and works efficiently with large amounts of dataset, making it suitable for a huge dataset [33]. DL is of great interest because of its superior accuracy when training with a large volume of data, as it is considered the most powerful classification technique among all machine learning methods. From 2012 to 2017, Champion always won the ImageNet competition in DL approach and in particular the CNN [12]. The famous method that used in systems is CNN that representing neurons into two dimensions used to detect and classify an object and a development of Multi-Layer Perceptron (MLP), CNN is characterized by having hidden layers in addition to the input and output layer. The benefit of these hidden layers is that they minimize errors between input and output by adjusting the weights of the values by using back-propagation. The general structure of CNN contains 3 layers [2] as in Figure 13 [34], namely Convolution Layer, Pooling Layer and Fully Connected Layer [2]. As well as, there are other additional layers in CNN, namely Bottleneck Layer, The sequential or sequential layer, Dropout Layer, Soft-max Layer and Transfer Learning [2].

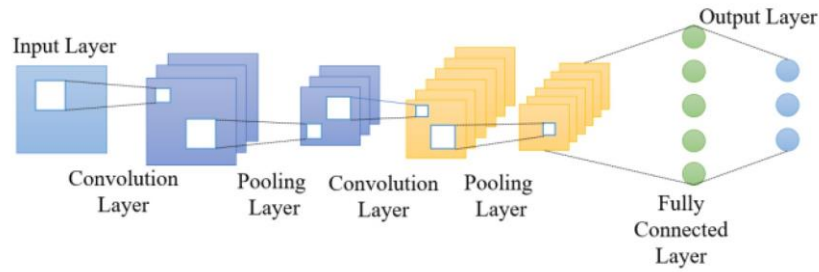


Figure 13. Basic general structure of CNN [34].

#### IV. DISCUSSION

According to Table 1, which contains the information of the diagnostic systems reviewed in this research paper. The difference in the accuracy of the systems can be observed according to the different types of methodology used in the image processing that precedes the classification process. This difference in methodology is due to the limitations of the images used by the systems. It can also be noted that there are few diagnostic systems for many diseases, such as cancers. Thus, there is a lack in studying the impact of the ROI in the iris of many organs, such as the breast and the brain.

On other hand can noted that the most commonly used classification method is machine learning, as in Figure 14. This is because the dataset available for eye images that are used to diagnose some diseases is limited, and not large enough to need to use deep learning to design diagnostic systems. And another most commonly used model of machine learning are SVM and back-propagation neural network as shown in Figure 15. So, the most widely used model for deep learning is CNN, as shown in Figure 16, which shows the highest accuracy according to the three types of classification model. Thus, it was found that the highest accuracy (99.92%) of the diagnostic system was based on machine learning using ELM model.

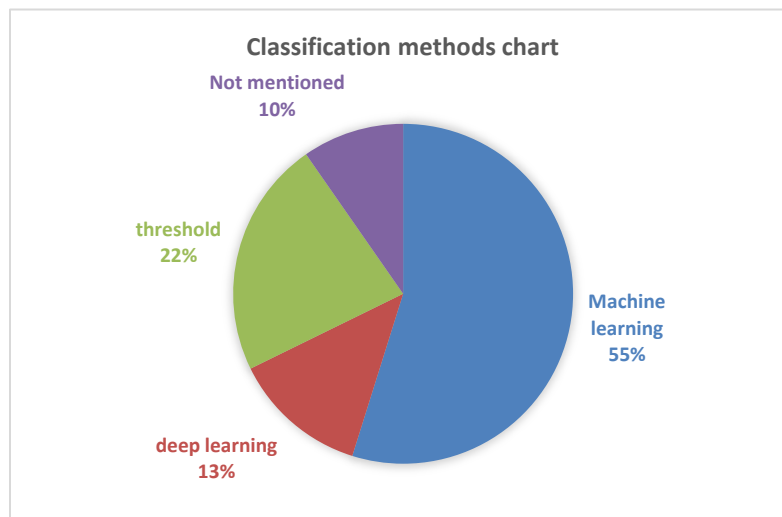


Figure 14. The Classification methods chart according to Table 1

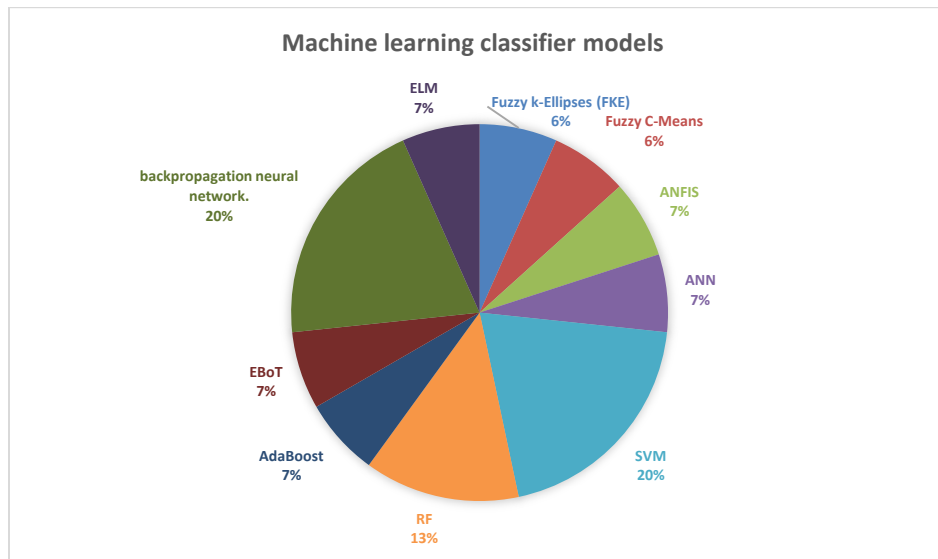


Figure 15. The Machine learning Classifier types chart that used in researches according to Table 1

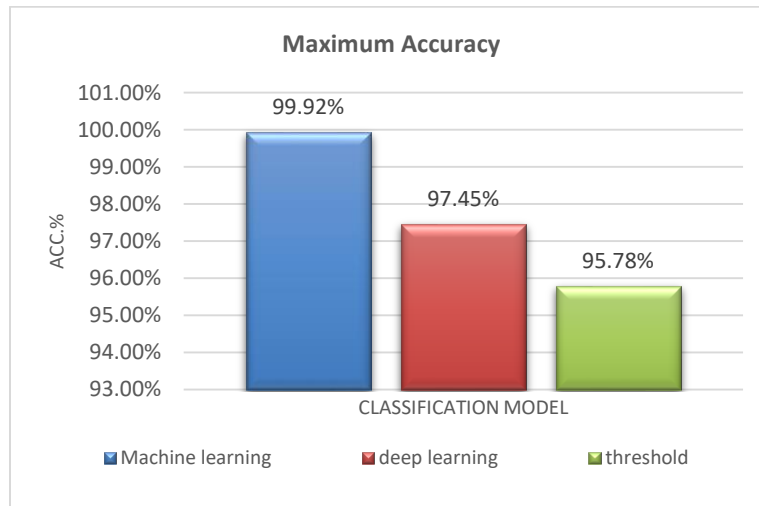


Figure 16. The chart of maximum accuracy of classification models that used in researches according to Table 1

## V. CONCLUSION

Research in complementary medical diagnostics, particularly in iris-based disease detection, has demonstrated the potential of leveraging image processing, computer vision, and artificial intelligence. Recent trends emphasize the increasing adoption of machine learning and deep learning techniques, often used in combination, due to their effectiveness in analyzing medical images. These approaches not only increase diagnostic accuracy but also reduce training time and enhance interface responsiveness.

Preprocessing of iris images prior to AI-based classification is a critical step in improving system efficiency. Challenges, however, remain, especially in the areas of iris segmentation and auto-cropping, often arising from variations in lighting and image capture conditions.

## VI. APPENDIX

### Table 1 Key:

**Acc.:** Accuracy, **Thr.:** Threshold, **ML:** Machine Learning, **DL:** Deep Learning, **IDL:** Interactive Data Language, **V.:** version, **HT:**Hough Transform, **CHT:** Circular Hough Transform, **IDO:** Integral Differential Operator, **DWT:** Discrete Wavelet Transform, **GLCM:** Grey Level Co-occurrence Matrix, **HOG:** Histogram of Oriented Gradients, **LBP:** Local Binary Pattern, **CLAHE:** Contrast limited adaptive histogram equalization, **GMM:** Gaussian mixture model, **FKE:** Fuzzy k-Ellipses, **ANFIS:** Adaptive Neuro-Fuzzy Inference system, **SVM:** Support Vector Machine, **BT:** Binary Tree Model, **RF:** Random Forest, **AB or AdaBoost:** Adaptive

Boosting Model, **GL**: Generalized Linear Models, **NN**: Neural Network Model, **LDA**: Linear Discriminative Analysis, **CNN**: Convolutional Neural Network, **ResNet**: Residual Neural Network, **DenseNet**: Dense Convolutional Network, **MSE**: Mean Square Error, **DT**: Decision Trees, **NB**: Naive Bayes, **KNN**: k-Nearest Neighbor, **ELM**: Extreme Learning Machine, **Adam**: Adaptive Moment, **Kiosk**: desktop application that can be used at Healthcare Kiosk, **Giresun Uni.**: Giresun University Health Practice and Research Hospital Cardiology Polyclinic, **IIMCT-Pakistan**: IIMCT-Pakistan Railway Hospital and NIRM-National Institute of Rehabilitation Medicine, **Bahawal Victoria Hos.**: Surgical Section I, Bahawal Victoria Hospital, Pakistan.

## REFERENCES

- [1] S. P. Jogi and B. B. Sharma, "Retracted: Methodology of iris image analysis for clinical diagnosis," in *2014 International Conference on Medical Imaging, m-Health and Emerging Communication Systems (MedCom)*, IEEE, Nov. 2014, pp. 235–240. doi: 10.1109/MedCom.2014.7006010.
- [2] C. Banowati, A. Novianty, and C. Setianingsih, "Cholesterol Level Detection Based on Iris Recognition Using Convolutional Neural Network Method," in *2019 IEEE Conference on Sustainable Utilization and Development in Engineering and Technologies (CSUDET)*, IEEE, Nov. 2019, pp. 116–121. doi: 10.1109/CSUDET47057.2019.9214690.
- [3] Z. Othman and A. Satria Prabuwono, "Retracted: Preliminary study on iris recognition system: Tissues of body organs in iridology," in *2010 IEEE EMBS Conference on Biomedical Engineering and Sciences (IECBES)*, IEEE, Nov. 2010, pp. 115–119. doi: 10.1109/IECBES.2010.5742211.
- [4] R. A. Ramlee and S. Ranjit, "Retracted: Using Iris Recognition Algorithm, Detecting Cholesterol Presence," in *2009 International Conference on Information Management and Engineering*, IEEE, Apr. 2009, pp. 714–717. doi: 10.1109/ICIME.2009.61.
- [5] T. Hussain *et al.*, "Retracted: An Iris based Lungs Pre-diagnostic System," in *2019 2nd International Conference on Computing, Mathematics and Engineering Technologies (iCoMET)*, IEEE, Jan. 2019, pp. 1–5. doi: 10.1109/ICOMET.2019.8673495.
- [6] A. Bansal, R. Agarwal, and R. K. Sharma, "Pre-Diagnostic Tool to Predict Obstructive Lung Diseases Using Iris Recognition System," 2019, pp. 71–79. doi: 10.1007/978-981-10-8968-8\_7.
- [7] C.-L. Lai and C.-L. Chiu, "Retracted: Health examination based on iris images," in *2010 International Conference on Machine Learning and Cybernetics*, IEEE, Jul. 2010, pp. 2616–2621. doi: 10.1109/ICMLC.2010.5580885.
- [8] F. Hidayanti, H. Hadi Santoso, and H. Endo Prasetyo, "Upper Stomach Disorder Detection System using Back-propagation Artificial Neural Network," *International Journal of Emerging Trends in Engineering Research*, vol. 8, no. 8, pp. 4426–4432, Aug. 2020, doi: 10.30534/ijeter/2020/62882020.
- [9] K. Sivasankar, M. Sujaritha, P. Pasupathi, and S. Muthukumar, "Retracted: FCM based iris image analysis for tissue imbalance stage identification," in *2012 International Conference on Emerging Trends in Science, Engineering and Technology (INCOSSET)*, IEEE, Dec. 2012, pp. 210–215. doi: 10.1109/INCOSSET.2012.6513907.
- [10] S. E. Hussein, O. A. Hassan, and M. H. Granat, "Assessment of the potential iridology for diagnosing kidney disease using wavelet analysis and neural networks," *Biomed Signal Process Control*, vol. 8, no. 6, pp. 534–541, Nov. 2013, doi: 10.1016/j.bspc.2013.04.006.
- [11] L. F. Salles and M. J. P. da Silva, "The sign of the Cross of Andreas in the iris and Diabetes Mellitus: a longitudinal study," *Revista da Escola de Enfermagem da USP*, vol. 49, no. 4, pp. 0626–0631, Aug. 2015, doi: 10.1590/S0080-623420150000400013.
- [12] Y.-H. Li, M. S. Aslam, K.-L. Yang, C.-A. Kao, and S.-Y. Teng, "Classification of Body Constitution Based on TCM Philosophy and Deep Learning," *Symmetry (Basel)*, vol. 12, no. 5, p. 803, May 2020, doi: 10.3390/sym12050803.
- [13] D. H. Hareva, S. Lukas, and N. O. Suharta, "Retracted: The smart device for healthcare service: Iris diagnosis application," in *2013 Eleventh International Conference on ICT and Knowledge Engineering*, IEEE, Nov. 2013, pp. 1–6. doi: 10.1109/ICTKE.2013.6756277.
- [14] A. Bansal, R. Agarwal, and R. K. Sharma, "Determining diabetes using iris recognition system," *Int J Diabetes Dev Ctries*, vol. 35, no. 4, pp. 432–438, Dec. 2015, doi: 10.1007/s13410-015-0296-1.
- [15] M. A. R. Sitorus, M. H. Purnomo, and A. D. Wibawa, "Retracted: Iris image analysis of patient Chronic Renal Failure (CRF) using watershed algorithm," in *2015 4th International Conference on Instrumentation, Communications, Information Technology, and Biomedical Engineering (ICICI-BME)*, IEEE, Nov. 2015, pp. 54–58. doi: 10.1109/ICICI-BME.2015.7401334.
- [16] K. E. Martiana, A. R. Barakbah, S. S. Akmilis, and A. A. Hermawan, "Retracted: Application for heart abnormalities detection through Iris," in *2016 International Electronics Symposium (IES)*, IEEE, Sep. 2016, pp. 315–322. doi: 10.1109/ELECSYM.2016.7861024.

- [17] P. Samant and R. Agarwal, "Diagnosis of Diabetes Using Computer Methods: Soft Computing Methods for Diabetes Detection Using Iris," *International Journal of Medical, Health, Biomedical, Bioengineering and Pharmaceutical Engineering*, vol. 11, no. 2, pp. 63–68, 2017, doi: 10.5281/zenodo.1129721.
- [18] P. Samant and R. Agarwal, "Machine learning techniques for medical diagnosis of diabetes using iris images," *Comput Methods Programs Biomed*, vol. 157, pp. 121–128, Apr. 2018, doi: 10.1016/j.cmpb.2018.01.004.
- [19] P. Moradi, N. Nazer, A. K. Ahmadi, H. Mohammadzade, and H. K. Jafari, "Retracted: Discovering Informative Regions in Iris Images to Predict Diabetes," in *2018 25th National and 3rd International Iranian Conference on Biomedical Engineering (ICBME)*, IEEE, Nov. 2018, pp. 1–6. doi: 10.1109/ICBME.2018.8703564.
- [20] P. Samant and R. Agarwal, "Analysis of computational techniques for diabetes diagnosis using the combination of iris-based features and physiological parameters," *Neural Comput Appl*, vol. 31, no. 12, pp. 8441–8453, Dec. 2019, doi: 10.1007/s00521-019-04551-9.
- [21] P. A. Reshma, K. V. Divya, and T. B. Subair, "Detection of Heart Abnormalities and High-Level Cholesterol Through Iris," 2019, pp. 339–346. doi: 10.1007/978-3-030-00665-5\_35.
- [22] L. B. Rachman and Basari, "Detection of Cholesterol Levels by Analyzing Iris Patterns using Back-propagation Neural Network," *IOP Conf Ser Mater Sci Eng*, vol. 852, no. 1, p. 012157, Jul. 2020, doi: 10.1088/1757-899X/852/1/012157.
- [23] S. Muzamil, T. Hussain, A. Haider, U. Waraich, U. Ashiq, and E. Ayguadé, "An Intelligent Iris Based Chronic Kidney Identification System," *Symmetry (Basel)*, vol. 12, no. 12, p. 2066, Dec. 2020, doi: 10.3390/sym12122066.
- [24] C. Yohannes, I. Nurtanio, and K. C. Halim, "Potential of Heart Disease Detection Based on Iridology," *IOP Conf Ser Mater Sci Eng*, vol. 875, no. 1, p. 012034, Jun. 2020, doi: 10.1088/1757-899X/875/1/012034.
- [25] H. A. U. Rehman, C. Y. Lin, and S. F. Su, "Deep learning based chronic kidney disease detection through iris," *J Phys Conf Ser*, vol. 2020, no. 1, p. 012047, Sep. 2021, doi: 10.1088/1742-6596/2020/1/012047.
- [26] E. M. Kusumaningtyas, A. Barakbah, and S. Dangriawan, "Diabetes and Heart Disease Identification System Using Iris on the Healthcare Kiosk," *J Phys Conf Ser*, vol. 1811, no. 1, p. 012096, Mar. 2021, doi: 10.1088/1742-6596/1811/1/012096.
- [27] S. K. Punia, M. Kumar, S. K. Pathak, and X. Cheng, "Diabetes and heart disease identification using biomedical iris data," *Applied and Computational Engineering*, vol. 2, no. 1, pp. 336–345, Mar. 2023, doi: 10.54254/2755-2721/2/20220676.
- [28] F. Özbilgin, Ç. Kurnaz, and E. Aydın, "Prediction of Coronary Artery Disease Using Machine Learning Techniques with Iris Analysis," *Diagnostics*, vol. 13, no. 6, p. 1081, Mar. 2023, doi: 10.3390/diagnostics13061081.
- [29] S. J. Wagh, "WFL Publisher Android mobile application for heart abnormality disease detection through human iris," 2023, doi: 10.1234/4.2023.5749.
- [30] C. Fernandez-Grandon, I. Soto, and D. Zabala-Blanco, "Extreme Learning Machine for Iris-Based Diabetes Detection," in *2023 IEEE CHILEAN Conference on Electrical, Electronics Engineering, Information and Communication Technologies (CHILECON)*, IEEE, Dec. 2023, pp. 1–6. doi: 10.1109/CHILECON60335.2023.10418742.
- [31] M. Jawad Kathem and T. Salman Atia, "A Review on IoT Cyber-Attacks Detection Challenges and Solutions," *Al-Iraqia Journal of Scientific Engineering Research*, vol. 2, no. 3, pp. 22–31, Aug. 2023, doi: 10.58564/IJSER.2.3.2023.84.
- [32] E. Najjar and A. Majeed Breesam, "Supervised Machine Learning a Brief Survey of Approaches," *Al-Iraqia Journal of Scientific Engineering Research*, vol. 2, no. 4, pp. 71–82, Jan. 2024, doi: 10.58564/IJSER.2.4.2023.121.
- [33] A. Mubashra, A. Naeem, Dr. N. Aslam, M. K. Abid, and J. Haider, "Diabetic Retinopathy Identification from Eye Fundus images using Deep Features," *VFAST Transactions on Software Engineering*, vol. 11, no. 2, pp. 172–186, Jun. 2023, doi: 10.21015/vtse.v11i2.1206.
- [34] H. Gu, Y. Wang, S. Hong, and G. Gui, "Blind Channel Identification Aided Generalized Automatic Modulation Recognition Based on Deep Learning," *IEEE Access*, vol. 7, pp. 110722–110729, 2019, doi: 10.1109/ACCESS.2019.2934354.